Polarization invariance in a Young interferometer

Massimo Santarsiero[1,*]

[1]*Università Roma Tre, Dipartimento di Fisica, and Consorzio Nazionale Interuniversitario per le Scienze Fisiche della Materia, Via della Vasca Navale 84, I-00146 Rome, Italy*
**Corresponding author: santarsiero@fis.uniroma3.it*

Received June 4, 2007; accepted August 14, 2007;
posted September 4, 2007 (Doc. ID 83685); published October 12, 2007

Conditions ensuring that the polarization properties at the output plane of a Young interferometer fed by an electromagnetic partially coherent beam are the same as those at the pinholes are derived. Such a behavior is interpreted in terms of the vector modes of the electromagnetic source corresponding to the field emerging from the Young pinholes. © 2007 Optical Society of America

OCIS codes: 030.1640, 260.5430, 260.2110, 120.3180.

1. INTRODUCTION

The effects on the polarization features of the electromagnetic field across the output plane of a Young interferometer due to the correlations existing between the fields emerging from the two pinholes of the mask have been the subject of several recent works [1–7].

It has been shown, in particular, that the elements of the polarization matrix [8] of the field across the output plane of the interferometer may differ from those of the field at the pinholes as the result of a generalized interference law [1] involving the second-order correlations between the field components at the pinholes. This happens even when the fields at the two points present identical local polarization properties. As a consequence, the degree of polarization [2,4], as well as the Stokes parameters [5,6], may present an oscillating behavior across the interference pattern and generally differ from those of the impinging field. Theoretical predictions about the effects of coherence on the on-axis polarization degree in a Young interferometer were experimentally confirmed in [9].

In the present paper, the conditions assuring that the polarization properties of the field at any point across the fringe pattern are the same as those at the pinholes will be determined. It will be assumed that the fields at the pinholes are characterized by polarization matrices that are mutually proportional, so that the two fields present the same polarization features but may carry different powers. Such an invariance condition will be shown to be reflected onto the form of the 4×4 matrix comprising all the second-order correlations among the field components at the pinholes [3,7].

The behavior of the field across the output plane of the interferometer will then be interpreted by using the tools provided by the modal theory of coherence for vector fields [10,11], according to which any partially coherent electromagnetic source can be thought of as the superposition of a certain number, possibly infinite, of mutually uncorrelated, perfecly correlated, and polarized field distributions. While, in general, the problem of the mode determination in the vector case is a very difficult task to be solved analytically, it becomes much simpler when the source consists of a pair of points in the space (a so-called two-point source), as is the case for the radiation emerging from the holes of an ideal Young mask [3,7]. As we shall see, it turns out to be quite elementary if the above polarization-invariance condition is assumed.

The paper is organized as follows. In Section 2 the theoretical background of the modal theory of coherence for electromagnetic beams is breifly recalled, together with its application to two-point sources. The invariance condition is then derived in Section 3, while general properties of the pertinent modal expansion are discussed in Section 4. Finally, a detailed analysis is given in Section 5 under simplifying assumptions about the values of the source parameters.

2. PRELIMINARIES

The complete set of the second-order, space-time correlation functions of the electromagnetic field at two points can be described, in the paraxial limit, by the beam coherence–polarization (BCP) matrix [1,12], defined as the correlation between the Jones vectors of the fields at the two points. More precisely, if one introduces the Jones vector of the electric field at the coordinate $\mathbf{r}$ as the column vector

$$\mathbf{E}(\mathbf{r},t)=\begin{pmatrix}E_x(\mathbf{r},t)\\ E_y(\mathbf{r},t)\end{pmatrix}, \tag{1}$$

the corresponding BCP matrix at points $\mathbf{r}_1$ and $\mathbf{r}_2$ is defined as

$$\hat{J}(\mathbf{r}_1,\mathbf{r}_2)=\langle\mathbf{E}(\mathbf{r}_1,t)\mathbf{E}^{\dagger}(\mathbf{r}_2,t)\rangle=\begin{bmatrix}J_{xx}(\mathbf{r}_1,\mathbf{r}_2) & J_{xy}(\mathbf{r}_1,\mathbf{r}_2)\\ J_{yx}(\mathbf{r}_1,\mathbf{r}_2) & J_{yy}(\mathbf{r}_1,\mathbf{r}_2)\end{bmatrix}, \tag{2}$$

where the dagger denotes Hermitian conjugation and the angle brackets time average. In the case of polychromatic radiation a cross-spectral density (CSD) tensor in the spectral domain can be defined [13], but the two definitions are equivalent if quasi-mochromatic sources are considered. Accordingly, although in the following we shall use the definition given in Eq. (2), our results could be easily transposed in the space–frequency domain.

The local polarization properties of the beam are specified by the BCP matrix evaluated with $\mathbf{r}_1=\mathbf{r}_2$, which coincides with the polarization (or coherence) matrix defined in [8]. In particular, the optical intensity and the degree of polarization at the coordinate $\mathbf{r}$ turn out to be

$$I(\mathbf{r}) = \mathrm{Tr}\{\hat{J}(\mathbf{r},\mathbf{r})\} \tag{3}$$

and

$$P(\mathbf{r}) = \sqrt{1 - \frac{4\mathrm{Det}\{\hat{J}(\mathbf{r},\mathbf{r})\}}{[\mathrm{Tr}\{\hat{J}(\mathbf{r},\mathbf{r})\}]^2}}, \tag{4}$$

respectively, where Det stands for determinant and Tr for trace.

Some years ago, a modal theory of coherence for electromagnetic partially coherent fields was presented [10,11] as an extension of the well-known Wolf's scalar theory [14]. According to the former, any partially polarized, partially coherent source can be thought of as obtained from the incoherent superposition of a discrete, possibly infinite, number of perfectly correlated and perfectly polarized fields (the *modes*), the power carried by each mode being proportional to a suitably evaluated *eigenvalue*.

Vector modes and eigenvalues are obtained by solving the following system of coupled integral equations:

$$\int \hat{J}(\mathbf{r}_1,\mathbf{r}_2)\boldsymbol{\Phi}_n(\mathbf{r}_2)\mathrm{d}\mathbf{r}_2 = \Lambda_n \boldsymbol{\Phi}_n(\mathbf{r}_1), \tag{5}$$

where $\boldsymbol{\Phi}_n(\mathbf{r})$ represents the Jones vector of the nth modes and Λ_n its eigenvalue. Because of the nonnegative character of $\hat{J}(\mathbf{r}_1,\mathbf{r}_2)$, it turns out that $\Lambda_n \geqslant 0$ for any n. Furthermore, from the definition of vector modes, a Mercer expansion can be used to represent the BCP matrix, namely,

$$\hat{J}(\mathbf{r}_1,\mathbf{r}_2) = \sum_n \Lambda_n \boldsymbol{\Phi}_n(\mathbf{r}_1)\boldsymbol{\Phi}_n^{\dagger}(\mathbf{r}_2). \tag{6}$$

The determination of the modal structure becomes quite simple in the case of two-point sources, that is, when only a pair of source points at a time is of interest, as is the case for the radiation emerging from the pinholes of the mask of a Young interferometer. In fact, the modes and the corresponding eigenvalues of a two-point source can be evaluated by solving the secular problem for a 4×4 complex-valued matrix [3,7]. To show this, we represent the electric field vectors at the points $\mathbf{p}_1$ and $\mathbf{p}_2$ of the mask plane by four-component column vectors, namely,

$$\mathrm{E}(t) = \begin{pmatrix} \mathbf{E}_1(t) \\ \mathbf{E}_2(t) \end{pmatrix} = \begin{pmatrix} E_x^{(1)}(t) \\ E_y^{(1)}(t) \\ E_x^{(2)}(t) \\ E_y^{(2)}(t) \end{pmatrix}, \tag{7}$$

where $\mathbf{E}_i(t)(i=1,2)$ denotes the Jones vector of the transverse electromagnetic field at the point located at $\mathbf{p}_i$, and $E_\alpha^{(i)}(t)$ $(\alpha=x,y)$ are its cartesian components. Accordingly, a 4×4 correlation matrix, say $\hat{\rho}$, can be defined as

$$\hat{\rho} = \langle \mathrm{E}(t)\mathrm{E}^{\dagger}(t)\rangle = \begin{bmatrix} \hat{J}_{11} & \hat{J}_{12} \\ \hat{J}_{12}^{\dagger} & \hat{J}_{22} \end{bmatrix}, \tag{8}$$

where $\hat{J}_{ij}=\langle \mathbf{E}_i(t)\mathbf{E}_j^{\dagger}(t)\rangle$ $(i,j=1,2)$ is the BCP matrix evaluated at the points i and j, and eigenvalues and modes of the two-point source are evaluated from the secular problem for the matrix $\hat{\rho}$, that is [7],

$$\hat{\rho}\boldsymbol{\Psi}_n = \lambda_n \boldsymbol{\Psi}_n. \tag{9}$$

In Eq. (9), the vector $\boldsymbol{\Psi}_n$ contains the field components of the nth mode at the two pinholes, i.e.,

$$\boldsymbol{\Psi}_n = \begin{pmatrix} \boldsymbol{\Phi}_{n,1} \\ \boldsymbol{\Phi}_{n,2} \end{pmatrix} = \begin{pmatrix} \varphi_{n,x}^{(1)} \\ \varphi_{n,y}^{(1)} \\ \varphi_{n,x}^{(2)} \\ \varphi_{n,y}^{(2)} \end{pmatrix}, \tag{10}$$

while the eigenvalue λ_n is given by Λ_n/S, with S being a constant having dimensions of a surface and related to the actual size of the pinholes [7].

Since the BCP matrix is nonnegative definite [1], there will be four nonnegative eigenvalues and four mutually orthogonal eigenvectors, and a Mercer's expansion can be written for the matrix $\hat{\rho}$ as

$$\hat{\rho} = \sum_{n=1}^{4} \lambda_n \boldsymbol{\Psi}_n \boldsymbol{\Psi}_n^{\dagger}. \tag{11}$$

From a physical point of view, each of the modes represents a perfectly correlated field distribution at the pinholes, and any field distribution at the pinholes can be obtained by incoherently superimposing such four modes. More precisely, one needs at most four modes because, in certain cases, one or more eigenvalues may vanish. This means, in particular, that all the characteristics of the radiation across the observation plane can be deduced from a superposition scheme involving the vector modes of the BCP matrix at the pinholes. In fact, since the modes are mutually uncorrelated, the polarization matrix at the coordinate ξ in the observation plane can be written as the sum of the polarization matrices produced by each of the modes.

3. INVARIANCE CONDITION

Let us consider a Young interferometer fed by an electromagnetic field described by its own BCP matrix, and denote by $\mathbf{E}_1$ and $\mathbf{E}_2$ the random variables representing the Jones vectors of the electric field at the two pinholes.

The Jones vector of the field at the output plane of the interferometer will be of the form

$$\mathbf{E}_{\mathrm{out}}(\xi) = \mathbf{E}_1 e^{\mathrm{i}K\xi} + \mathbf{E}_2 e^{-\mathrm{i}K\xi}, \tag{12}$$

where inessential proportionality factors, as well as the explicit dependence on time, have been omitted, ξ is the transverse coordinate, and K gives account of the geometry of the system and is related to the period of the fringe pattern.

The BCP matrix at two points of the output plane can be expressed in terms of the above Jones vector as follows:

$$\hat{J}_{\text{out}}(\xi_1,\xi_2) = \langle \mathbf{E}_{\text{out}}(\xi_1)\mathbf{E}^{\dagger}_{\text{out}}(\xi_2)\rangle, \tag{13}$$

the local properties of the output field being evaluated by letting $\xi_1=\xi_2=\xi$, in which case the BCP matrix reduces to the polarization matrix.

We want to determine the conditions under which the local polarization properties of the output field are exacly the same as those at the pinholes. Of course, such a requirement makes sense only when the polarization matrices of the field at the two pinholes are proportional to each other. If we denote by $\hat{J}_{11}$ and $\hat{J}_{22}$ such matrices, we then require $\hat{J}_{11}=\alpha\hat{P}$ and $\hat{J}_{22}=\beta\hat{P}$, with $\hat{P}$ being a *bona fide* polarization matrix, i.e., a Hermitian positive semidefinite 2×2 matrix. We can write $\hat{P}$ in the form

$$\hat{P} = \begin{bmatrix} a & c \\ c^* & b \end{bmatrix}, \tag{14}$$

where a and b are real quantities greater then or equal to zero and c is a complex number such that, from the Schwartz inequality, $|c|^2 \leqslant ab$.

Let us now evaluate $\hat{J}_{\text{out}}(\xi,\xi)$. From Eqs. (13) and (12) we have

$$\hat{J}_{\text{out}}(\xi,\xi) = \langle \mathbf{E}_1\mathbf{E}_1^{\dagger}\rangle + \langle \mathbf{E}_2\mathbf{E}_2^{\dagger}\rangle + \langle \mathbf{E}_1\mathbf{E}_2^{\dagger}\rangle e^{2\mathrm{i}K\xi} + \langle \mathbf{E}_2\mathbf{E}_1^{\dagger}\rangle e^{-2\mathrm{i}K\xi}$$
$$= \hat{J}_{11} + \hat{J}_{22} + \hat{J}_{12}e^{2\mathrm{i}K\xi} + \hat{J}^{\dagger}_{12}e^{-2\mathrm{i}K\xi}, \tag{15}$$

so that it is evident that the only way to have $\hat{J}_{\text{out}}(\xi,\xi)$ proportional to $\hat{P}$ for any choice of the coordinate ξ is taking $\hat{J}_{12}=\gamma\hat{P}$, with γ being a complex number. In such a way, the polarization matrix across the fringe plane turns out to be

$$\hat{J}_{\text{out}}(\xi,\xi) = (\alpha+\beta+2\mathrm{Re}\{\gamma e^{2\mathrm{i}K\xi}\})\hat{P}, \tag{16}$$

and the normalized Stokes parameters, as well as the degree of polarization, at any point of the fringe plane are the same as those present at the Young holes.

The parameters α, β, and γ cannot take arbitrary values because of the constraints imposed on the elements of polarization matrices. In particular, since the diagonal elements of $\hat{J}_{11}$ and $\hat{J}_{22}$ must be real and positive, α and β must be real and positive, too. Furthermore, the modulus of γ is bounded by the Schwartz inequality. In fact, if we consider a typical element, say $J^{12}_{\ell k}(\ell,k=x,y)$ of the matrix $\hat{J}_{12}$, the Schwartz inequality requires $|J^{12}_{\ell k}|^2 \leqslant J^{11}_{\ell\ell}J^{22}_{kk}$ so that, as can be easily verified, it must be that $|\gamma|^2\leqslant\alpha\beta$. It should be noted that, because of such constraints, the quantity in parentheses in Eq. (16) is always nonnegative.

The intensity across the fringe plane is obtained by taking the trace of $\hat{J}_{\text{out}}(\xi,\xi)$ and turns out to be

$$I_{\text{out}}(\xi) = (\alpha+\beta+2\mathrm{Re}\{\gamma e^{2\mathrm{i}K\xi}\})(a+b), \tag{17}$$

which is independent of the polarization state of the field at the pinholes and coincides, up to the proportionality factor $(a+b)$, with the intensity distribution that would have been obtained from the interference of two scalar fields having intensities α and β, respectively, and mutual intensity γ.

In conclusion, the conditions we have found for the polarization invariance across the fringe pattern are: $\hat{J}_{11}=\alpha\hat{P}$, $\hat{J}_{22}=\beta\hat{J}_{\text{P}}$, and $\hat{J}_{12}=\gamma\hat{P}$. This means that the 4×4 correlation matrix representing the two-point source at the pinholes consists of four blocks proportional to one another and therefore can be written as

$$\hat{\rho} = \hat{\rho}_{\text{S}} \otimes \hat{P}, \tag{18}$$

where

$$\hat{\rho}_{\text{S}} = \begin{bmatrix} \alpha & \gamma \\ \gamma^* & \beta \end{bmatrix}, \tag{19}$$

and $\otimes$ denotes the tensor, or Kronecker, product [15]. When a matrix $\hat{\rho}$ can be written in the form of Eq. (18), it is said to be *factorizable*. From the above constraints about the values of the elements of $\hat{\rho}_{\text{S}}$ it follows that the latter is also a Hermitian positive semidefinite matrix. The subscript "S" stands for "scalar" because the matrix $\hat{\rho}_{\text{S}}$ is just the 2×2 correlation matrix that would have been obtained in the study of the modal structure of a scalar two-point source, following an approach similar to that of [3,7].

A direct consequence of the condition in Eq. (18) is that any partially coherent electromagnetic field whose BCP matrix can be written in the form [11]

$$\hat{J}(\mathbf{r}_1,\mathbf{r}_2) = J_{\text{S}}(\mathbf{r}_1,\mathbf{r}_2)\hat{P}, \tag{20}$$

with J_{S} being a scalar mutual intensity function, exhibits polarization invariance across the output plane when it feeds a Young interferometer, wherever the two pinholes are located. We then have $\alpha=J_{\text{S}}(\mathbf{p}_1,\mathbf{p}_1)$, $\beta=J_{\text{S}}(\mathbf{p}_2,\mathbf{p}_2)$, and $\gamma=J_{\text{S}}(\mathbf{p}_1,\mathbf{p}_2)$, where $\mathbf{p}_1$ and $\mathbf{p}_2$ are the position vectors of the holes.

From Eq. (18) it is seen that the polarization properties of such sources are somewhat decoupled from their coherence properties. Such a decoupling will be made more evident when considering the modal expansion of sources of this kind.

4. MODAL EXPANSION OF FACTORIZABLE $\hat{\rho}$ MATRICES

The evaluation of the modal structure of the two-point source is particularly simple in those cases where the corresponding $\hat{\rho}$ matrix is expressible as the Kronecker product of two 2×2 matrices, i.e., when

$$\hat{\rho} = \hat{\rho}_{\text{S}} \otimes \hat{P} = \begin{bmatrix} \alpha & \gamma \\ \gamma^* & \beta \end{bmatrix} \otimes \begin{bmatrix} a & c \\ c^* & b \end{bmatrix}, \tag{21}$$

where $\hat{\rho}_{\text{S}}$ and $\hat{P}$ are Hermitian and positive semidefinite.

When this happens, in fact, eigenvalues and eigenvectors of $\hat{\rho}$ are given by suitable products of the corresponding quantities of the two smaller matrices, and can always be calculated by solving two second-order secular equations. Nevertheless, as we saw above, significant two-point sources belong to the present class.

A. Modal Structure of the Two Submatrices

Let us consider first eigenvalues and modes of the matrix $\hat{\rho}_{\mathrm{S}}$. As stated above, they determine the modal structure of a s calar two-point source. The eigenvalues are easily evaluated as

$$\lambda_1^{\mathrm{S}} = \tfrac{1}{2}[(\alpha+\beta) + \sqrt{(\alpha-\beta)^2 + 4|\gamma|^2}],$$

$$\lambda_2^{\mathrm{S}} = \tfrac{1}{2}[(\alpha+\beta) - \sqrt{(\alpha-\beta)^2 + 4|\gamma|^2}], \tag{22}$$

which the following eigenvectors correspond to:

$$\boldsymbol{\Psi}_1^{\mathrm{S}} = N_{\mathrm{S}}\begin{pmatrix} \eta_{\mathrm{S}} e^{\mathrm{i}\psi_{\mathrm{S}}} \\ 1 \end{pmatrix}, \quad \boldsymbol{\Psi}_2^{\mathrm{S}} = N_{\mathrm{S}}\begin{pmatrix} e^{\mathrm{i}\psi_{\mathrm{S}}} \\ -\eta_{\mathrm{S}} \end{pmatrix}; \tag{23}$$

where ψ_{S} is the argument of the complex number γ, while

$$\eta_{\mathrm{S}} = \frac{(\alpha-\beta) + \sqrt{(\alpha-\beta)^2 + 4|\gamma|^2}}{2|\gamma|}, \tag{24}$$

represents the unbalancing between the field amplitudes of the modes at the two points, and

$$N_{\mathrm{S}} = \frac{1}{\sqrt{1+\eta_{\mathrm{S}}^2}}. \tag{25}$$

is a normalization factor.

According to the modal theory of coherence, any scalar two-point source can be thought of as the incoherent superposition of the above two modes, which represent perfectly coherent field distributions at the two points. The amplitudes of the modes at the two holes are just the elements of the vectors in Eq. (23), while their powers are given by the corresponding eigenvalues. With reference to a Young interferometer scheme, it is also true that any interference pattern can be considered as produced from the superposition of two mutually uncorrelated patterns, each of them obtained from one of the modes.

We stress that such two patterns do not present, in general, unitary visibility, because of the presence of the unbalancing factor η_{S}, which depends on the elements of $\hat{\rho}_{\mathrm{S}}$, and is unitary only when $\alpha=\beta$. However, a general characteristic of such modes, which follows from their orthogonality, is that they always produce two interference patterns that are in phase opposition at the output plane of the interferometer, as can be also directly verified from Eq. (23). In particular, we may write

$$I_{1,2}^{\mathrm{S}}(\xi) = \lambda_{1,2}^{\mathrm{S}} N_{\mathrm{S}}^2[1 + \eta_{\mathrm{S}}^2 \pm 2\eta_{\mathrm{S}}\cos(2K\xi + \psi_{\mathrm{S}})], \tag{26}$$

where the + (−) sign has to be chosen for the first (second) mode.

Analogous considerations hold, of course, for $\hat{P}$, and the expressions for λ_i^{P} and $\boldsymbol{\Psi}_i^{\mathrm{P}}$ $(i=1,2)$ exactly correspond to those in Eqs. (22) and (23). In this case, however, we are dealing with the modal structure of a polarization matrix of a field at a fixed point, and the modes now represent the Jones vectors of two perfectly polarized fields whose superposition gives rise to the field at that point. The eigenvalues give the power contribution of the two modes, while the orthogonality between the modes means exactly that their polarization states are mutually orthogonal.

B. Modal Structure of the Composite Matrix

Eigenvalues and eigenvectors of the composite matrix are given by [15]

$$\lambda_1 = \lambda_1^{\mathrm{S}}\lambda_1^{\mathrm{P}}, \quad \lambda_2 = \lambda_1^{\mathrm{S}}\lambda_2^{\mathrm{P}},$$

$$\lambda_3 = \lambda_2^{\mathrm{S}}\lambda_1^{\mathrm{P}}, \quad \lambda_4 = \lambda_2^{\mathrm{S}}\lambda_2^{\mathrm{P}}; \tag{27}$$

$$\boldsymbol{\Psi}_1 = \boldsymbol{\Psi}_1^{\mathrm{S}} \otimes \boldsymbol{\Psi}_1^{\mathrm{P}}, \quad \boldsymbol{\Psi}_2 = \boldsymbol{\Psi}_1^{\mathrm{S}} \otimes \boldsymbol{\Psi}_2^{\mathrm{P}},$$

$$\boldsymbol{\Psi}_3 = \boldsymbol{\Psi}_2^{\mathrm{S}} \otimes \boldsymbol{\Psi}_1^{\mathrm{P}}, \quad \boldsymbol{\Psi}_4 = \boldsymbol{\Psi}_2^{\mathrm{S}} \otimes \boldsymbol{\Psi}_2^{\mathrm{P}}. \tag{28}$$

Some important consequences arise from such a modal structure. First, for each of the modes the electric fields at the two points have the same polarization state, coincident with the polarization state of one of the eigenvectors of $\hat{P}$. More precisely, the modes $\boldsymbol{\Psi}_1$ and $\boldsymbol{\Psi}_3$ are polarized as $\boldsymbol{\Psi}_1^{\mathrm{P}}$ while $\boldsymbol{\Psi}_2$ and $\boldsymbol{\Psi}_4$ are polarized as $\boldsymbol{\Psi}_2^{\mathrm{P}}$, which is orthogonal to the former. Second, the phase difference between the fields at the two holes is ψ_{S} for the first two modes, as it happens for $\boldsymbol{\Psi}_1^{\mathrm{S}}$, while it is $\psi_{\mathrm{S}}+\pi$ for the last two, as for $\boldsymbol{\Psi}_2^{\mathrm{S}}$. This means that the interference patterns produced across the output plane of the Young interferometer by $\boldsymbol{\Psi}_1$ and $\boldsymbol{\Psi}_2$ are exactly superimposed, being proportional to the intensity profile I_1^{S} [see Eq. (26)]. The same happens to the fringes produced by $\boldsymbol{\Psi}_3$ and $\boldsymbol{\Psi}_4$, but the pertinent intensity distribution is proportional to I_2^{S}, which is laterally shifted by half a period with respect to I_1^{S}. Typical intensity distributions of the fringe pattern produced by the four modes are shown in Fig. 1 where, for simplicity, the phase ψ_{S} has been set to zero.

The above considerations help one understand the behavior of the interference pattern as far as its polarization properties are concerned. In fact, since the modes are superimposed incoherently, the whole polarization matrix at the coordinate ξ can be written as the sum of the polarization matrices pertinent to each of the modes. In particular, some of the features, such as the total intensity and the degree of polarization across the interference pattern, can be directly deduced from the equations derived above. The total intensity is evaluated by summing all contributions and using Eqs. (22)–(27), while the polarization degree across the fringe pattern, $P_{\mathrm{out}}(\xi)$, is easily deduced if one considers that the modes $\boldsymbol{\Psi}_1$ and $\boldsymbol{\Psi}_3$ have orthogonal polarization with respect to $\boldsymbol{\Psi}_2$ and $\boldsymbol{\Psi}_4$. This means that $P_{\mathrm{out}}(\xi)$ can be evaluated as

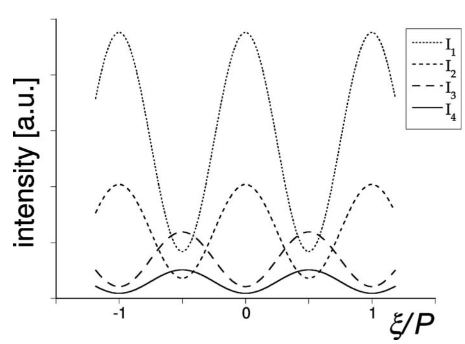

Fig. 1. Typical intensity distributions produced across the output plane by the four modes. The phase ψ_{S} has been set to zero and $P=\pi/K$ denotes the fringe period.

$$P_{\mathrm{out}}(\xi) = \frac{|[I_1(\xi)+I_3(\xi)]-[I_2(\xi)+I_4(\xi)]|}{I_1(\xi)+I_2(\xi)+I_3(\xi)+I_4(\xi)} = \frac{|\lambda_1^{\mathrm{P}}-\lambda_2^{\mathrm{P}}|}{\lambda_1^{\mathrm{P}}+\lambda_2^{\mathrm{P}}}, \tag{29}$$

which is independent of the spatial coordinate and, as is required, equals that at the pinholes. We want to remark that the key features of the modal structure that are responsible for such behavior are the orthogonality of the polarization states of the modes and the fact that $\lambda_1/\lambda_2 = \lambda_3/\lambda_4$, so that at any point of the fringe pattern the ratio between the powers of the component polarized as $\mathbf{\Psi}_1^{\mathrm{P}}$ and that polarized in the orthogonal way is constant.

In Section 5 we shall apply the results presented here, adopting simplyfing assumptions about the parameters of the source, so that simpler explicit expressions for modes and eigenvalues will be obtained.

5. EXAMPLE

From the results of Section 3, we know that a two-point source described by the matrix in Eq. (30) produces radiation with uniform polarization across the output plane of a Young interferometer. It may be interesting to analyze in some detail such behavior in terms of the coherent mode decomposition of the source. This could be done without any restrictions on the parameters of the two-point source but, to simplify the expressions to come and the pertinent figures, we take $\alpha=\beta$, which means that the fields at the the two Young pinholes carry the same power. Furthermore, we take γ and c as real nonnegative quantities. By the way, such conditions can be always be fulfilled in practice, provided that a suitable absorbing element and suitable retarders are placed in front of one of the two holes. Without any loss of generality, we further assume $a \geqslant b$.

The matrix in Eq. (21) can then be written as

$$\hat{\rho} = \alpha \begin{bmatrix} 1 & \mu \\ \mu & 1 \end{bmatrix} \otimes \begin{bmatrix} a & c \\ c & b \end{bmatrix}, \tag{30}$$

where μ is the scalar degree of coherence between the holes, defined as $\gamma/\sqrt{\alpha\beta}$. We may immediately evaluate the intensity of the fields emerging from each of the pinholes, i.e.,

$$I_{\mathrm{ph}} = \alpha(a+b), \tag{31}$$

and the polarization degree at the pinholes, that is,

$$P_{\mathrm{ph}} = \frac{\sqrt{(a-b)^2+4c^2}}{(a+b)}. \tag{32}$$

Eigenvalues and eigenvectors of $\hat{\rho}$ are readily obtained from Eqs. (22)–(28) as

$$\lambda_1 = \alpha(1+\mu)[(a+b)+\sqrt{(a-b)^2+4c^2}],$$

$$\lambda_2 = \alpha(1+\mu)[(a+b)-\sqrt{(a-b)^2+4c^2}],$$

$$\lambda_3 = \alpha(1-\mu)[(a+b)+\sqrt{(a-b)^2+4c^2}],$$

$$\lambda_4 = \alpha(1-\mu)[(a+b)-\sqrt{(a-b)^2+4c^2}], \tag{33}$$

$$\mathbf{\Psi}_1 = \frac{N}{\sqrt{2}}\begin{pmatrix} \eta_{\mathrm{P}} \\ 1 \\ \eta_{\mathrm{P}} \\ 1 \end{pmatrix}, \quad \mathbf{\Psi}_2 = \frac{N}{\sqrt{2}}\begin{pmatrix} 1 \\ -\eta_{\mathrm{P}} \\ 1 \\ -\eta_{\mathrm{P}} \end{pmatrix},$$

$$\mathbf{\Psi}_3 = \frac{N}{\sqrt{2}}\begin{pmatrix} \eta_{\mathrm{P}} \\ 1 \\ -\eta_{\mathrm{P}} \\ -1 \end{pmatrix}, \quad \mathbf{\Psi}_4 = \frac{N}{\sqrt{2}}\begin{pmatrix} 1 \\ -\eta_{\mathrm{P}} \\ -1 \\ \eta_{\mathrm{P}} \end{pmatrix}; \tag{34}$$

respectively, where

$$\eta_{\mathrm{P}} = \frac{(a-b)+\sqrt{(a-b)^2+4c^2}}{2c}, \tag{35}$$

$$N = \frac{1}{\sqrt{1+\eta_{\mathrm{P}}^2}}. \tag{36}$$

As was expected, the polarization states of the modes follow the ones of the polarization matrix $\hat{P}$ and are therefore independent of μ, i.e., of the correlation existing between the two Young pinholes. In particular, since c has been taken as real, the polarizations of the modes are linear. The latter are sketched in Fig. 2, where the arrow directions highlight the phase relations existing for each mode between the fields at the pinholes.

It is interesting to note that the polarization angle ϑ depends only on the quantity $(a-b)/c$. More precisely, from Eqs. (34) and (35) we have

$$\vartheta = \tan^{-1}\left(\frac{1}{\eta_{\mathrm{P}}}\right) = \tan^{-1}\left[\frac{(a-b)}{2c} + \sqrt{1+\left(\frac{a-b}{2c}\right)^2}\right]^{-1}, \tag{37}$$

so that it tends to 0 when $(a-b)/c \to \infty$ (and this happens when $a \gg b$ or when $c \to 0$) while it goes to $\pi/4$ when $a \to b$ (see Fig. 3).

As far as the eigenvalues are concerned, their values depend also on μ. A typical behavior of the four eigenvalues as functions of μ is shown in Fig. 4.

The two limiting cases of $\mu \to 1$ and $\mu \to 0$ are of particular interest and are worth being considered in some detail, starting from the first one.

If $\mu \simeq 1$, the corresponding components of the electric field at the two Young pinholes are perfectly correlated

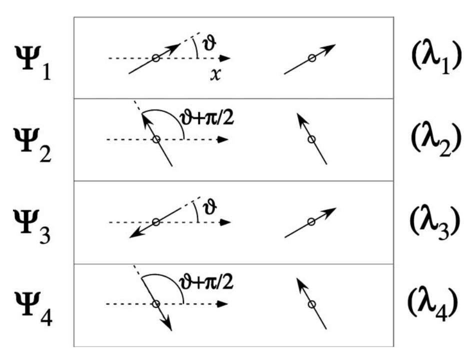

Fig. 2. Polarization of the modes at the two Young pinholes for the source of Section 5.

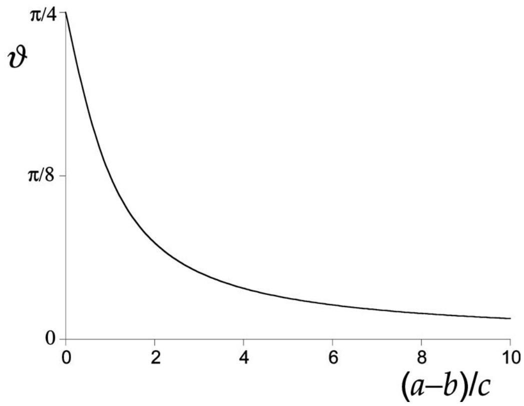

Fig. 3. Polarization direction of $\boldsymbol{\Psi}_1$ for the source of Section 5.

and we expect fringes with maximum visibility across the output plane. In such a limit, from Eq. (33), two of the eigenvalues (namely, λ_3 and λ_4) vanish, which means that only two modes (namely, $\boldsymbol{\Psi}_1$ and $\boldsymbol{\Psi}_2$) are required, at most, to describe the BCP of the field emerging from the pinholes. One mode is sufficient if λ_2 vanishes, too, and this happens if $c^2=a$, i.e., when the incident field is fully polarized.

On the observation plane both the modes give rise to an intensity distribution of the form $I_i(\xi)\propto\lambda_i\cos^2(K\xi+\psi_S/2)$ $\times(i=1,2)$, and this explains why the visibility of the overall pattern turns out to be unitary. Moreover, since the two modes are linearly polarized along mutually orthogonal directions, the degree of polarization as a function of ξ can be evaluated at once as

$$P_{\text{out}}(\xi)=\frac{I_1(\xi)-I_2(\xi)}{I_1(\xi)+I_2(\xi)}=\frac{\lambda_1-\lambda_2}{\lambda_1+\lambda_2}=\frac{\sqrt{(a-b)^2+4c^2}}{(a+b)}, \quad (38)$$

which is uniform across the plane and equal to that at the pinholes, as was expected.

In the opposite limit ($\mu\simeq 0$) there is no correlation at all between the field components at the two pinholes, and we expect that the problem of the mode determination reduces to two independent problems, one for each of the pinholes. In fact, if $\mu=0$, we see from Eq. (33) that $\lambda_1=\lambda_3$ and $\lambda_2=\lambda_4$. As a result of such degeneracies, different modes can be chosen as linear combinations of $\boldsymbol{\Psi}_1$ and $\boldsymbol{\Psi}_3$ (and of $\boldsymbol{\Psi}_2$ and $\boldsymbol{\Psi}_4$). In particular, one can choose

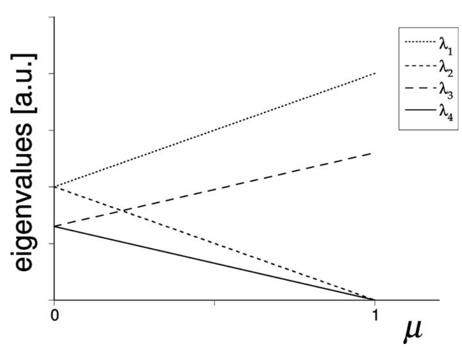

Fig. 4. Four eigenvalues as functions of the scalar degree of coherence between the fields at the Young pinholes for the source of Section 5.

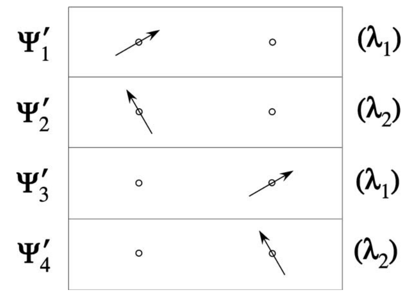

Fig. 5. Polarization of the modes at the two Young pinholes for the case of the source of Section 5 with $\mu\simeq 0$.

$$\boldsymbol{\Psi}_1'=\frac{\boldsymbol{\Psi}_1+\boldsymbol{\Psi}_3}{\sqrt{2}}=N\begin{pmatrix}\eta_P\\1\\0\\0\end{pmatrix},$$

$$\boldsymbol{\Psi}_2'=\frac{\boldsymbol{\Psi}_2+\boldsymbol{\Psi}_4}{\sqrt{2}}=N\begin{pmatrix}1\\-\eta_P\\0\\0\end{pmatrix},$$

$$\boldsymbol{\Psi}_3'=\frac{\boldsymbol{\Psi}_1-\boldsymbol{\Psi}_3}{\sqrt{2}}=N\begin{pmatrix}0\\0\\\eta_P\\1\end{pmatrix},$$

$$\boldsymbol{\Psi}_4'=\frac{\boldsymbol{\Psi}_2-\boldsymbol{\Psi}_4}{\sqrt{2}}=N\begin{pmatrix}0\\0\\1\\-\eta_P\end{pmatrix}. \quad (39)$$

The problem of the mode determination indeed reduces to two independent problems, and for each of the modes, field is present only on one of the two pinholes (see Fig. 5). Since the polarization matrices of the fields at the two holes are identical, their eigenvalues and modes are exactly the same. In particular, even when the incident beam is fully polarized, there cannot be fewer than two (degenerate) modes in the expansion.

No fringes are observed across the output plane of the interferometer because no one of the modes gives rise to interference fringes, so that the intensity visibility of the overall pattern is zero. As far as the polarization properties of the output field are concerned, we simply note that the latter can be thought of as consisting of two mutually uncorrelated contributions having orthogonal polarizations and powers proportional to λ_1 and λ_2, respectively, so that exactly the same result as in Eq. (38) is obtained.

6. CONCLUSIONS

When an electromagnetic partially coherent light source is used as the input of a Young interferometer, the polarization properties of the field across the interference pattern are generally different from those of the field impinging on the Young mask, even when the local polarization properties of the input field are identical at the two holes. In the present paper, the conditions assuring that the polarization properties of the input field are preserved across the output plane have been derived within the framework of the paraxial approximation. Such a requirement has been shown to affect the form of the 4×4 correlation matrix comprising the second-order correlations between all the possible pairs of transverse components of the electric field at the two pinholes. It turns out that such matrix has to be expessible as the tensor product of two submatrices to account for the polarization of the source and its coherence properties, respectively.

The structure of the interference pattern has then been interpreted in terms of the modes of the partially coherent electromagnetic source representing the field emerging from the Young holes. All the coherence–polarization features of the interference pattern of a Young interferometer, in fact, can be deduced from a superposition scheme involving four mutually uncorrelated, perfectly polarized, and correlated electromagnetic fields. In the case of polarization invariance, it has been shown that such modes, together with the correspoding eigenvalues, are evaluated in closed analytical form by solving the secular problems for two 2×2 Hermitian matrices.

Results presented here find application in the study of the two-beam interference of vector fields but, more in general, they could give a deeper insight into the relationship between the polarization of an electromagnetic light source and its spatial-coherence properties.

ACKNOWLEDGMENTS

The author wishes to thank R. Borghi and F. Gori for helpful discussions during the preparation of the manuscript.

REFERENCES

1. F. Gori, M. Santarsiero, S. Vicalvi, R. Borghi, and G. Guattari, “Beam coherence polarization matrix,” Pure Appl. Opt. **7**, 941–951 (1998).
2. H. Roychowdhury and E. Wolf, “Young's interference experiment with light of any state of coherence and polarization,” Opt. Commun. **252**, 268–274 (2005).
3. F. Gori, M. Santarsiero, and R. Borghi, “Vector mode analysis of a Young interferometer,” Opt. Lett. **31**, 858–860 (2006).
4. Y. Li, H. Lee, and E. Wolf, “Spectra, coherence and polarization in Young's interference pattern formed by stochastic electromagnetic beams,” Opt. Commun. **265**, 63–72 (2006).
5. T. Setälä, J. Tervo, and A. T. Friberg, “Stokes parameters and polarization contrasts in Young's interference experiment,” Opt. Lett. **31**, 2208–2210 (2006).
6. A. Luis, “Ray picture of polarization and coherence in a Young interferometer,” J. Opt. Soc. Am. A **23**, 2855–2860 (2006).
7. M. Santarsiero, F. Gori, R. Borghi and G. Guattari, “Vector-mode analysis of symmetric two-point sources,” J. Opt. A, Pure Appl. Opt. **9**, 593–602 (2007).
8. L. Mandel and E. Wolf, *Optical Coherence and Quantum Optics* (Cambridge U. Press, 1995).
9. F. Gori, M. Santarsiero, R. Borghi, and E. Wolf, “Effects of coherence on the degree of polarization in Young interference pattern,” Opt. Lett. **31**, 688–690 (2006).
10. F. Gori, M. Santarsiero, R. Simon, G. Piquero, R. Borghi, and G. Guattari, “Coherent-mode decomposition of partially polarized, partially coherent sources,” J. Opt. Soc. Am. A **20**, 78–84 (2003).
11. J. Tervo, T. Setälä, and A. T. Friberg, “Theory of partially coherent electromagnetic fields in the space–frequency domain,” J. Opt. Soc. Am. A **21**, 2205–2215 (2004).
12. F. Gori, “Matrix treatment for partially polarized, partially coherent beams,” Opt. Lett. **23**, 41–43 (1998).
13. E. Wolf, “Unified theory of coherence and polarization of statistical electromagnetic beams,” Phys. Lett. A **312**, 263–267 (2003).
14. E. Wolf, “New theory of partial coherence in the spacefrequency domain. I. Spectra and cross-spectra of steady-state sources,” J. Opt. Soc. Am. **72**, 343–351 (1982).
15. R. Horn and C. Johnson, *Topics in Matrix Analysis* (Cambridge U. Press, 1991), Chap. 4.